Studying the Effect of Delay Diversity on a DS-CDMA Downlink

Sumanth Jagannathan K.Giridhar
Department of Electrical Engineering
Indian Institute of Technology, Madras
Chennai, India 600036

Abstract

In this paper, we study the error rate performance of a direct sequence CDMA downlink similar to the CDMA2000 standard. While analytical computation of the error rate is possible in DS-CDMA systems under certain simplifying assumptions, computer simulations are perhaps the only means to quantify the error rate for realistic channel models. Since the delay spread of the multipath channel varies with distance, we investigate the error performance as a function of the distance from the base station. The computer simulations reveal certain interesting results which to our knowledge have not explicitly appeared in open literature. We compare the RAKE error rate performance under situations of no handoff, soft handoff, independent fading, correlated fading, chip-spaced sampling, sub-chip sampling, and pilot channel cancellation at the mobile receiver. These results indicate that narrow-band DS-CDMA downlink has certain severe shortcomings, and that it may be vital to ensure line of sight propagation for the "near" users and exploit base-station (macro) diversity for the "far" users (in soft handoff) to ensure adequate error rate performance.

Index Terms

DS-CDMA downlink, delay diversity, macro-cellular diversity, micro-cellular diversity, soft handoff.

I. Introduction

Traditionally, researchers have investigated the BER performance for different SNR's in a DS-CDMA system. This helps in understanding the performance of the DS-CDMA

system and in comparing various types of transmit/receive schemes. However, such a study is limited in the sense that a particular power delay profile is assumed for the channel irrespective of the distance of the mobile from the base station.

In a real DS-CDMA system, as a mobile moves towards or away from the base station, it experiences a variation in the channel. This variation is not due to fading alone but also due to the *delay spread* of the multipath channel. The delay spread of a multipath channel increases as the mobile moves away from the base station and therefore the channel taps vary in position as the mobile moves to or from the base station. Therefore, for a fixed SNR, the BER performance may vary depending on the distance of the mobile from the base station. In this paper, we model the delay spread and investigate the BER performance of the DS-CDMA system as a function of distance of the mobile from the base station. Since realistic channel models are used, we perform computer simulations to quantify the error rate performance.

The time diversity available due to the inherent characteristics of the multipath channel termed as *micro-cellular diversity* which however, may not be easy to exploit. First of all, the various paths of the multipath channel have to be chip-time resolvable, and secondly, since the channel may be arbitrarily spaced, the receiver must be able to estimate to the channel to a reasonable extent. Also, the diversity due to the delay spread of the channel can be exploited only if the channel taps are independent. Suppose the different channel taps are themselves correlated, there may not be any diversity in the channel that the receiver could make use of.

In a typical DS-CDMA system design, about 50% of the mobiles are in soft handoff. In such a case, the mobile will receive independent copies of the signal from the other base stations. This form of diversity called *macro-cellular diversity*, is a true diversity and will definitely lead to an improvement in performance. [1]

[1]However, field measurements have shown that too many base stations contributing to macro diversity may actually reduce performance (pilot leakage). Therefore, care should be taken to ensure that the mobile in soft handoff "sees" 2 or atmost 3 base stations.

In this paper, the performance improvement obtained from micro-cellular diversity and macro-cellular diversity is investigated. We have simulated the DS-CDMA downlink assuming a chip rate of $1.2288Mcps$ and the IS-95 base station specific scrambling code. An exponential power delay profile, a distance specific choice for delay spread and Rician K factor reducing exponentially with distance are assumed. Interesting insights into the DS-CDMA downlink performance are obtained through our simulations. We find that the line of sight component of the multipath channel is the dominant factor in determining the BER at distances near the base station. Near the edge of the cell site, the macro-cellular diversity available due to soft handoff becomes an important factor in reducing the BER.

This paper is organized as follows. The system model is described in Section II. The simulation results are given in Section III. Finally, some concluding remarks and suggestions for future research are given in Section IV.

II. System Model

We follow the problem formulation and symbol convention as in[5]. The complex baseband system model for the DS-CDMA downlink is illustrated in Figure 1.

A. The Transmitter

The downlink of a DS-CDMA system uses Walsh codes (Orthogonal codes) for channelization and spreading, and a short pseudo-orthogonal sequence or a Pseudo-Noise sequence (short PN sequence) for complex scrambling[1]. Each base station is assigned a unique shift on the code circle of the PN sequence. This helps in differentiating between the various base stations. In order to demultiplex the different channels at the receiver, each channel is assigned a unique Walsh code.

Figure 2 shows the spreading and modulation for a downlink user.

Let there be N channels (including $N-3$ user traffic channels and the pilot, sync and paging channels). Therefore, the desired traffic channel has $N-1$ interfering channels.

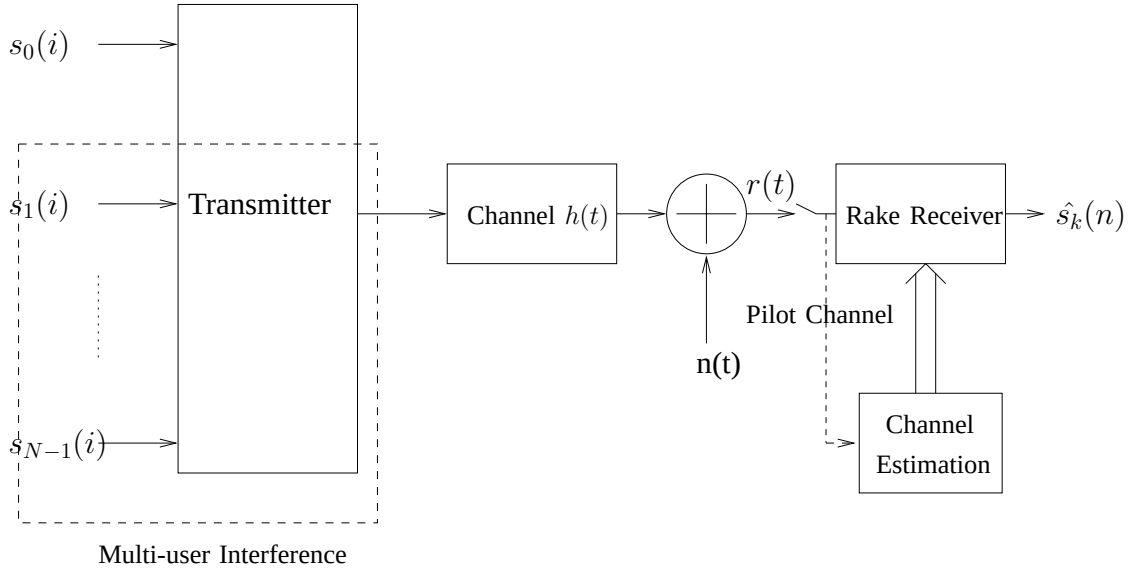

Figure 1. Complex baseband system model for the downlink of a DS-CDMA system

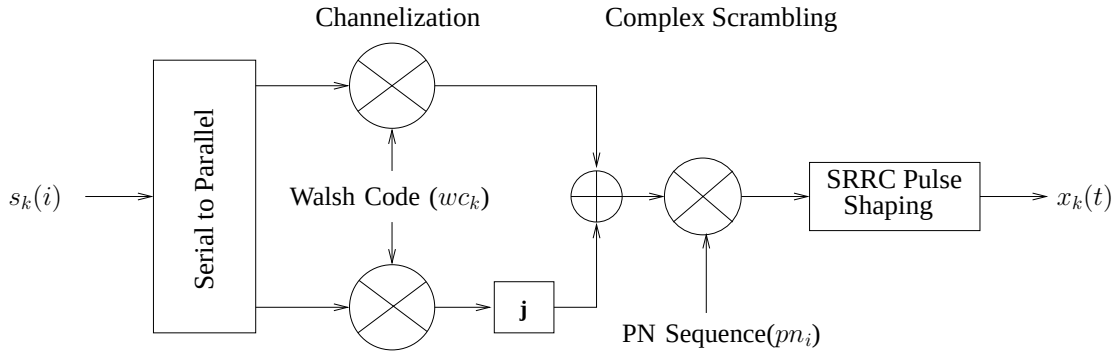

Figure 2. The transmitter block on the DS-CDMA downlink

The i^{th} data symbol for traffic channel k, $s_k(i)$ is spread using using the symbol-period-dependent spreading waveform $w_{k,i}(t)$. Hence, the transmitted signal of traffic channel k can be expressed as

$$x_k(t) = \sum_{i=-\infty}^{\infty} s_k(i) w_{k,i}(t - iT) \tag{1}$$

where T is the symbol duration. Each symbol is assumed to have unit amplitude; i.e.,

$$|s_k(i)|^2 = 1 \tag{2}$$

The spreading waveform for the k^{th} user and the i^{th} bit consists of a complex chip sequence, $c_{k,i}(j)$ convolved with the chip pulse shape (SRRC) $g(t)$, giving

$$w_{k,i}(t) = \frac{1}{\sqrt{SF}} \sum_{j=0}^{SF-1} c_{k,i}(j) g(t - jT_c) \tag{3}$$

where $c_{k,i}(j) = wc_k(j) * pn_i(j), \forall\ j = 0 : SF - 1$ and SF is the spreading factor.

1) Power distribution: The pilot, paging and synchronization channels are common to all the mobile stations and therefore a fixed amount of power is assigned to these channels so that they can be received without much error even at the edge of the cell site. The pilot channel is the most important in this regard as the channel estimation depends critically on the received pilot signal. Table I shows the typical distribution of the transmit power among the various channels on a DS-CDMA downlink.

TABLE I
Transmit power distribution among the various channels

Name of the channel	Percentage of transmit power
Pilot channel	20%
Paging channel	14%
Sync channel	2%
All Traffic channels	64%

2) The PN Sequence generator: The short PN sequence of IS-95 and CDMA2000[2] has a period of $2^{15}-1$ and an all zero code is inserted to make the period 2^{15}. The generator polynomial for the I-arm and the Q-arm short PN sequences are given respectively as:

$$P_I(x) = x^{15} + x^{13} + x^9 + x^8 + x^7 + x^5 + 1 \quad and \tag{4}$$

$$P_Q(x) = x^{15} + x^{12} + x^{11} + x^{10} + x^6 + x^5 + x^4 + x^3 + 1 \tag{5}$$

B. The Discrete Multipath Channel Model

A 5-tap fading multipath channel as shown in Figure 3 is considered. The channel is characterized by the following equivalent baseband impulse response

$$h(t) = \sum_{i=0}^{4} \alpha_i \delta(t - \tau_i) \tag{6}$$

where τ_i is the delay of the i^{th} tap of the multipath channel w.r.t the first tap ($\tau_0 = 0$) and α_i is the complex gain of that tap.

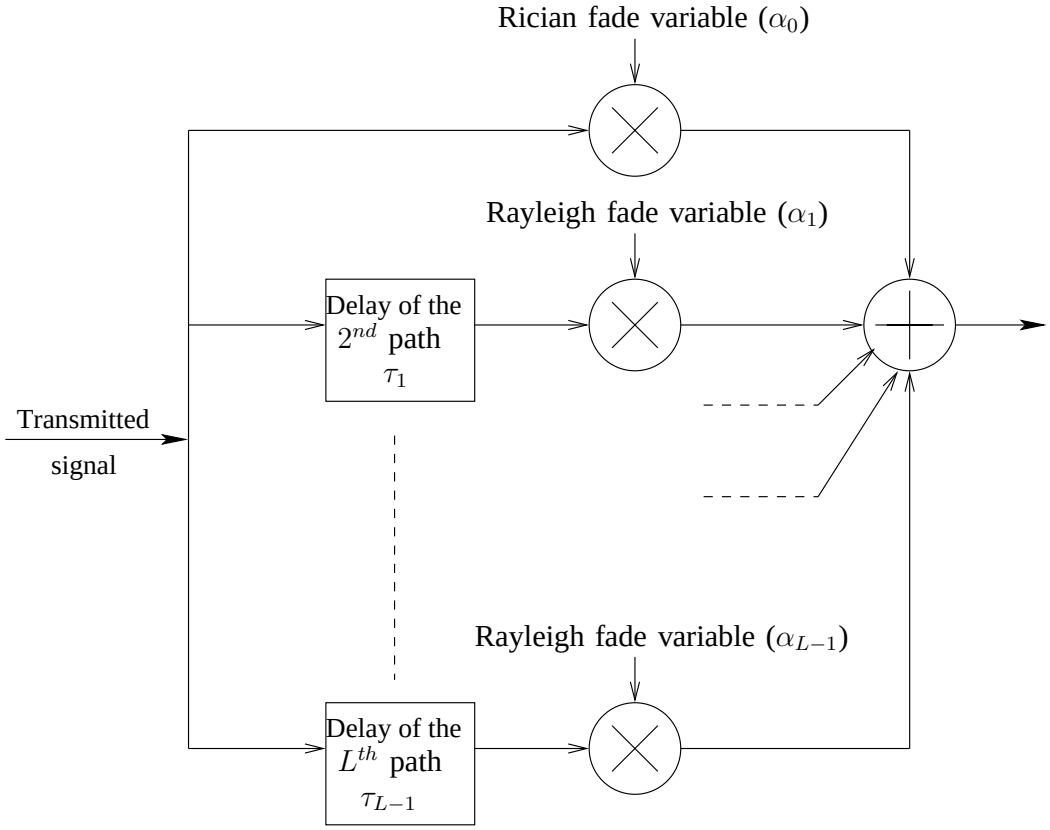

Figure 3. Time Varying Channel

We assume that the channel follows an exponential power delay profile given by the following equation.

$$p(\tau) = \exp(-\beta_0 \tau) \tag{7}$$

The power delay profile is limited to the -10dB level w.r.t to the maximum. If the maximum is 1, then the limit will be at 0.1. The delay at which a signal level of -10dB is received w.r.t the first path is denoted as $\Delta\tau$. The channel consists of 5 taps equally spaced from 0 to $\Delta\tau$ where time 0 corresponds to the first path that the mobile station encounters.

The exponential power delay profile is shown in Figure 4. The interval $\Delta\tau$ is split into 4 parts in order to obtain a 5-tap discrete time multipath channel. The first path is assumed to be a LoS Rician fading channel whereas the remaining 4 paths are taken as non-LoS Rayleigh fading channels.

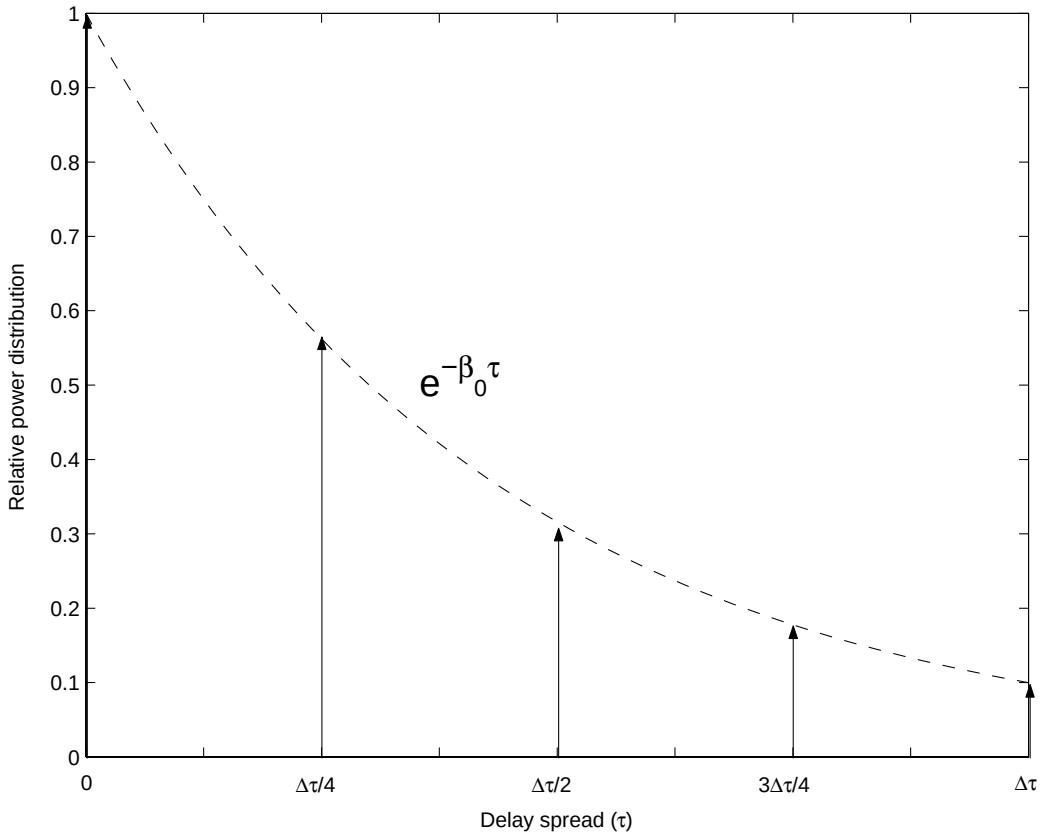

Figure 4. The Exponential Power Delay Profile for the Discrete Multipath Channel Impulse Response

1) Delay-spread model: As the mobile station goes further away from the base station, the transmitted wave undergoes more scattering in space and finally reaches the mobile

by means of multiple reflections. Therefore, one can expect a mobile that is farther away from the base station to see paths that are much more spread in time than one that is closer to the base station. This heuristic is captured in our delay spread model. $\Delta\tau$ is a measure of the delay-spread of the channel and is 20% of the propagation delay; i.e.,

$$\Delta\tau = 0.2 \times (d/c) \tag{8}$$

where d is the distance of the mobile from the base station and c is the speed of light.

Therefore, for a given distance from the base station we can obtain the 5-tap channel with the power delay profile parameter β_0 calculated from :

$$\beta_0 = (\ln 10)/\Delta\tau \tag{9}$$

2) Fading model: The Non Line of Sight (NLOS) paths are modelled as Rayleigh fading variables whose spectrum is given by Jake's model[6],[7]. The rayleigh fading simulator is described in[4]. The variance ($\sigma_i^2,\ \forall\ 0 \leq i \leq 4$) of the Rayleigh variables is obtained from the exponential power delay profile as

$$\sigma_i^2 = e^{-\beta_0 \cdot \tau_i} \tag{10}$$

When a Line of Sight (LOS) path is present, then a Rician fading model is adopted for that path[6],[7] with the mean of the fade variable being specified by a K parameter. The K parameter indicates that the power present in the LOS component of the Rician fading path is K times the power in the NLOS component. The Rician fade variable with a particular K parameter can be generated from the Rayleigh fade variable as shown in (11) where is the R Rician variable and J is the Rayleigh variable and σ_J is the power in the NLOS component.

$$R = \sqrt{K \cdot \sigma_J} + J \tag{11}$$

In our simulation, we assume the first path to be a LOS Rician fading channel with the other 4 channels being Rayleigh. For any given value of K say K_0, the line of sight component is assumed to decay exponentially from $K = K_0$ at $300m$ from the base station to $K = 0.1$ at $3km$ from the base station i.e the edge of the cell. This decay of the LOS component as a function of distance is given by

$$K(d) = K_0 \cdot e^{-B\cdot(d-300)} \tag{12}$$

where d is the distance of the mobile from the base station and

$$B = \frac{log(K_0/0.1)}{2700} \tag{13}$$

3) Correlated Channel Taps: Let the channel have 5 taps and let $X_i,\ \forall\ 1 \leq i \leq 5$ be 5 independent Rayleigh fade variables with unit energy. The channel taps positions are fixed at delays $\tau_i,\ \forall\ 1 \leq i \leq 5$ with the fade variable X_i corresponding to the delay τ_i. The 5 correlated channel taps $Y_j,\ \forall\ 1 \leq j \leq 5$ are generated from X_i as follows.

The fade variable Y_j corresponds to the delay τ_j and hence should be more correlated with X_j. Also, the correlation between Y_j and X_i must reduce as the time difference $|\tau_j - \tau_i|$ increases. Therefore we assume an exponential model for the magnitude correlation, $|\rho| = E[|Y_j||X_i^*|]$ as a function of $|\tau_j - \tau_i|$ while the phase correlation $\angle\rho$ is taken to be linear with $(\tau_j - \tau_i)$. $\angle\rho$ equals zero when $\tau_j = \tau_i$. The model also assumes a cut-off point of $10Tc$ at which we have $|\rho| = 0.01$. For a time difference more than $10Tc$, we assume that the paths are uncorrelated with each other.

Let $\tau = (\tau_j - \tau_i)$. Then we can define the magnitude correlation $|\rho|$ and the phase correlation $\angle\rho$ as follows.

$$|\rho| = exp(-\gamma|\tau|) \tag{14}$$

$$\angle\rho = \frac{\pi}{10Tc}(\tau) \tag{15}$$

where

$$\rho = E[Y_j X_i^*] \; \forall \; 1 \leq i, j \leq 5 \tag{16}$$

Thus the correlated taps Y_j are obtained from X_i by the following linear combination

$$\begin{bmatrix} Y_1 \\ Y_2 \\ \vdots \\ Y_L \end{bmatrix} = \begin{bmatrix} 1 & \rho_{12} & \rho_{13} & \dots & \rho_{1L} \\ \rho_{21} & 1 & \rho_{23} & \dots & \rho_{2L} \\ \vdots & & \ddots & & \vdots \\ \rho_{L1} & \rho_{L2} & \rho_{L3} & \dots & 1 \end{bmatrix} \begin{bmatrix} X_1 \\ X_2 \\ \vdots \\ X_L \end{bmatrix} \tag{17}$$

where

$$\rho_{ij} = E[Y_j X_i^*] \tag{18}$$

Finally, each variable $Y_i, \; \forall \; 1 \leq i \leq 5$ is normalized by the $\sum_{j=1}^{5} |\rho_{ij}|^2$ to ensure that the new fade variables are also of unit energy.

For generating correlated Rician fading channel taps, we need to first generate correlated Rayleigh fading variables and then add on a DC component to each variable depending on the corresponding K parameters.

4) Channel normalization: The channel is normalized such that the expected energy of the signal does not change when passed through it. This can be done as follows:

$$\sum_{i=0}^{4} E[\alpha_i \alpha_i^*] = 1; \tag{19}$$

Now for a Rayleigh variable α, $E[\alpha\alpha^*] = 2 \times \sigma^2$. Therefore in order to ensure a unit energy channel, we normalize all the fade variables by the following factor.

$$Normalizing factor = K \cdot \sigma_0^2 + 2 \sum_{i=0}^{4} \sigma_i^2 \tag{20}$$

C. DS-CDMA Receiver

The receiver structure after the signal is brought down to baseband consists of an SRRC (Square Root of Raised Cosine) filter followed by a chip-time or higher rate sampler. AWGN noise is added to the signal before the SRRC filter. An optimal way of performing pulse shaping and adding noise is discussed in[3]. This is followed by the de-spreader and de-scrambler. The channel estimation module runs parallely and estimates the mutli-path channel parameters using the incoming pilot signal. It is assumed that the mobile receiver is able to time synchronize with the base station and hence the propagation delay is not considered in our model. The different channels are demultiplexed and sent to the RAKE combiner along with the channel estimates. The typical receiver structure is illustrated in Figure 5.

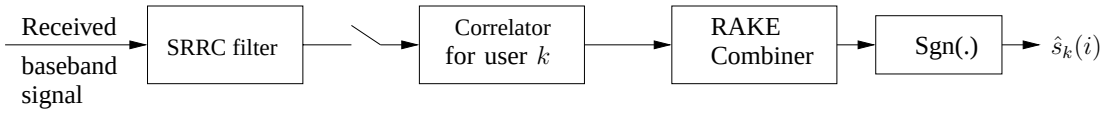

Figure 5. The receiver block on the DS-CDMA downlink

1) Channel Estimation: The conventional channel estimator as mentioned in[8] is adopted. The channel is estimated by correlating the received pilot signal with the complex conjugate of the PN sequence.

After performing the correlation, in order to ensure that we do not include many weak taps into our estimated channel, we set a threshold of say 3dB or 6dB i.e no tap that is more than 3dB/6dB weaker than the strongest tap will be included in the estimated channel. This is to prevent the weak taps (which may be spurious taps) from affecting the BER performance. At the same time, the threshold must be small enough to include genuine taps, which if ignored may once again deteriorate the performance.

Let $r(n)$ be the received signal after sampling, where n refers to the n^{th} chip. Let $c_{i,0} = pn_i * wc_0$ be the complex spreading sequence for the pilot channel where i refers to the i^{th} bit. $\bar{c}_{i,0}$ will be a vector consisting of SF(spreading factor) elements i.e

$[c_{1,i,0}\ c_{2,i,0}\ \ldots\ c_{j,i,0}\ \ldots\ c_{SF,i,0}]$. Let us assume that we estimate the channel till $5\times$Tc and that we perform the correlation over M bits.

Also, assume $\bar{c}_{i,0}^{M} = [\bar{c}_{i,0}\ \bar{c}_{i,0}\ \ldots\ M$ times$]$. To estimate the channel $\hat{h}_i$, we form the correlation matrix C_i as follows:

$$\bar{C}_i = \begin{bmatrix} \bar{c}_{1,i,0}^{M} & 0 & \ldots & 0 \\ \bar{c}_{2,i,0}^{M} & \bar{c}_{1,i,0}^{M} & & \vdots \\ \vdots & \bar{c}_{2,i,0}^{M} & \ddots & 0 \\ \bar{c}_{SF\cdot M,i,0}^{M} & \vdots & & \bar{c}_{SF\cdot M-5,i,0}^{M} \\ 0 & \bar{c}_{SF\cdot M,i,0}^{M} & & \bar{c}_{SF\cdot M-5+1,i,0}^{M} \\ \vdots & 0 & \ddots & \vdots \\ 0 & 0 & \ldots & \bar{c}_{SF\cdot M,i,0}^{M} \end{bmatrix} \tag{21}$$

We then form the received vector, $\bar{r} = [r\{i\cdot SF+1\}\ r\{(i+1)\cdot SF+1\}\ \cdots\ r\{(i+M)\cdot SF+1\}]^T$ and perform the correlation to estimate the channel as shown in (22).

$$\hat{h}_i = \frac{1}{\sqrt{P}\cdot(-1-j1)\cdot 2M\cdot SF}(\bar{C}_i^H\cdot\bar{r}) \tag{22}$$

where P is the transmit power of the Pilot channel.

2) Pilot Cancellation: One way of reducing interference at the receiver is through pilot cancellation. The pilot cancellation block is shown in Figure 6.

The channel is estimated at the mobile receiver in steps of Tc or $\frac{Tc}{2}$ from the received signal as described in section II-C.1. Since the pilot bits are known, the mobile estimates the received pilot channel based on the channel estimates and is cancelled from the received signal before sending it to the despreader and the RAKE receiver.

Pilot cancellation mainly helps only when the pilot signal is much stronger the traffic channel, in which case there is considerable amount of interference from the pilot channel. Cancelling this interference can improve performance. However, when the pilot strength is comparable to the strength of the traffic channel, the interference caused will

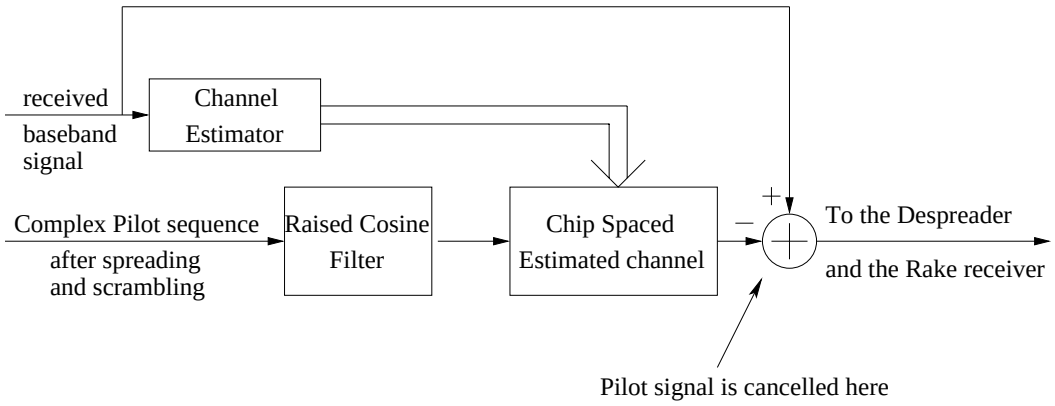

Figure 6. The Pilot cancellation block

not be very high and cancelling the pilot may even degrade the BER performance as the cancellation may occur at the wrong taps.

D. Cell site and delay spread

A circular cell site of radius $3km$ has been assumed. The BER is evaluated starting at a distance of 300m and continuing in steps of 300m till we reach the edge of the cell, i.e 3km. Table II shows the value of delay spread ($\Delta\tau$) for the various distances from the base station.

This shows that more chip-time resolvable paths are available as we move farther away from the base station. There is no delay-diversity available at a distance of $300m$ as all the taps are crowded within a quarter of a chip time whereas at the edge of the cell, we have 2 to 3 chip resolvable paths and this may lead to some diversity.

E. Model for Soft handoff

In order to simulate soft handoff, we assume two circular cell sites A and B of radius $3km$ each which are tangentially aligned as shown in Figure 7.

Let us consider a mobile in cell site A at different distances from the base station A. We assume that till a distance of $1800m$, the signal from base station B is not

TABLE II
Distance from BTS Vs Delay spread

Distance of mobile from the BTS	Delay spread
$600m$	$0.4915Tc$
$1200m$	$0.9830Tc$
$1800m$	$1.4746Tc$
$2400m$	$1.9661Tc$
$3000m$	$2.4576Tc$

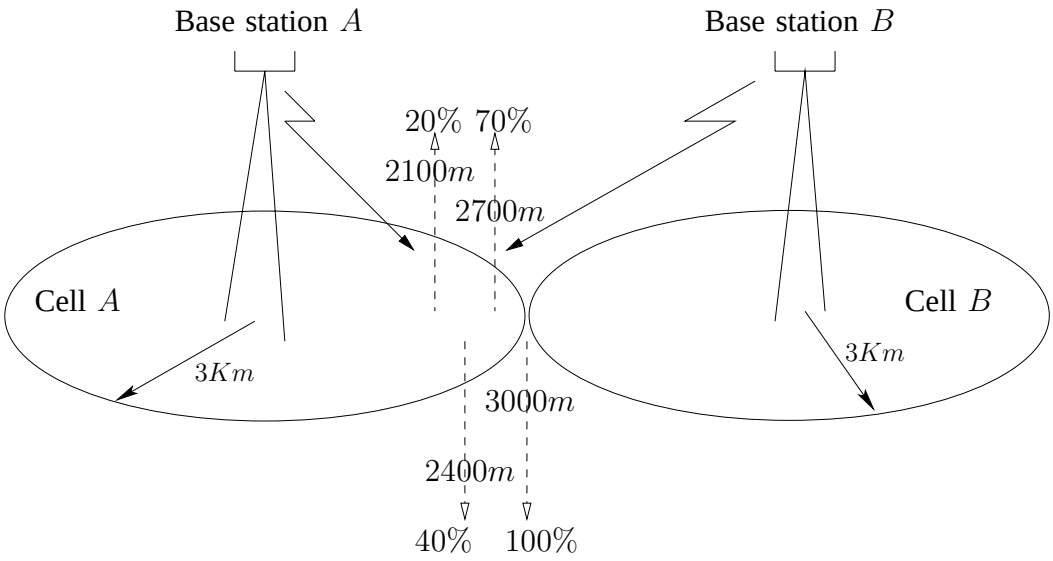

Figure 7. Cell arrangement in a two-way soft handoff. The value in $\%$ refers to the amount of power received by the mobile from base station B, keeping 100$\%$ power received from base station A as reference

strong enough and therefore the mobile is not in handoff. From a distance(d) of $2100m$ onwards, the mobile is in 2-way handoff. For $300m \leq d < 2100m$, the power received by the mobile from base station A is P and from base station B is 0. Table III shows the power received by the mobile from base stations A and B for $2100m \leq d \leq 3000m$.

III. Simulation Results

In this section, we present the error rate simulation results for the DS-CDMA down-link system. We present the variation of the BER as a function of the distance of the mobile from the base station under conditions of no handoff and soft handoff, correlated

TABLE III
Power received by a mobile in 2-way handoff

Distance of mobile from the BTS	Power from BTS A	Power from BTS B	Total power received
$2100m$	P	$0.2P$	$1.2P$
$240m$	P	$0.4P$	$1.4P$
$2700m$	P	$0.7P$	$1.7P$
$3000m$	P	P	$2P$

and independent fading and chip-rate and sub-chip correlation at the receiver. Also, the effect of pilot cancellation for different pilot strengths is observed. The optimized simulation models that were used in order to save simulation time are discussed in[9].

A. Simulation Parameters

The various parameters used in the simulation are given in Table IV.

TABLE IV
Simulation parameters

Parameter	Value
Number of bits used in the simulation	10^5
Speed of the mobile (Jake's spectrum)	$100\ Km/hr$
Carrier Frequency	$2\ GHz$
Data rate on Traffic channel	$19.2\ Kbps$
Chip rate (IS-95)	$1.2288\ Mcps$
Spreading factor	64
Transmit Signal to Interference ratio(SIR)	$-6dB/-9.5dB$
Number of channel taps	5
Received SNR ($\frac{Eb}{No}$)	$6dB$
Channel estimation window	$256\ chips$
Threshold for accepting RAKE fingers	$-3dB/-6dB$ w.r.t. strongest tap

The power distribution as mentioned in section II-A.1 is used for our simulations. Three traffic channels are simulated along with the pilot, sync and paging channels. Walsh codes 0, 1 and 32 are used for channelizing the Pilot, Paging and Sync channels,

respectively. The mobile speed of $100Km/hr$ corresponds to a Doppler spread (f_d) of $185Hz$. We also performed the simulations with a smaller doppler spread of $20Hz$. However, this did not lead to any significant improvement in the BER performance. This can be seen from Figure 8 where the BER curve for K=20 and f_d = 20Hz is compared with the curves obtained with f_d being 185Hz. All other results are shown for $f_d = 185Hz$.

B. Effect of the LoS path

Table V gives the BER tabulated for different values of the line of sight component K for the case of independent channel taps with a Tc-spaced correlator at the receiver. The value K refers to the LOS component at $300m$ from the base station. Irrespective of this initial value of K, the LOS component is assumed to decay to 0.1 at a distance of $3km$.

TABLE V
BER Vs Distance of the mobile from the base station for different values of K

Distance of the mobile from the base station	Line of Sight Component K			
	$K = 0$	$K = 6$	$K = 20$	$K = 100$
$300m$	1.30×10^{-1}	4.78×10^{-2}	1.63×10^{-2}	6.01×10^{-3}
$900m$	1.32×10^{-1}	8.07×10^{-2}	4.47×10^{-2}	1.36×10^{-2}
$1800m$	1.24×10^{-1}	1.09×10^{-1}	9.77×10^{-2}	7.79×10^{-2}
$2400m$	1.23×10^{-1}	1.16×10^{-1}	1.13×10^{-1}	1.12×10^{-1}
$3000m$	1.24×10^{-1}	1.20×10^{-1}	1.20×10^{-1}	1.21×10^{-1}

We can see an improvement in the BER performance as the line of sight path increases in strength. However at the edge of the cell ($3km$), we have assumed the line of sight component to be almost negligible. Therefore the BER converges to the case when all the channel taps are undergoing independent Rayleigh fading. Depending on the strength of the LOS component and the distance from the base station, the BER may even be an order better than the NLOS case. Thus we can conclude that the presence of a line of sight component definitely improves the BER.

C. Effect of Soft handoff

The soft handoff model as described in section II-E is implemented. A mobile in a soft handoff situation receives more interference than a mobile which is not in handoff. However, it also gains macro-cellular diversity from another base station. The signal received from the other base station is definitely fading independently from the signal coming from the closer base station. Therefore, the diversity obtained is a true diversity which leads to a considerable improvement in the BER performance.

Figures 8 and 9 show the BER versus Distance curves for the no handoff and soft handoff cases respectively for different values of the LOS component. The received SNR is fixed at $6dB$, the transmit SIR is $-6dB$ and the Rake acceptance threshold is $-3dB$. We can see that macro-cellular diversity helps in improving the BER performance at distances which are farther away from the base station and closer to the edge of the cell.

Further results in this thesis are shown under the following conditions:

1) The mobile receiver is in soft handoff.
2) The line of sight component(K) is 20.

D. Effect of correlated channel taps and sub-chip sampling at the receiver

From Figure 10, we can see that the BER performance in the case of correlated channel taps is worse than when the channel taps are independent. This is especially visible at distances farther away from the base station where the delay spread is higher and more chip resolvable paths exist. The reason for this is that when the channel taps are independent, the receiver is able to exploit the micro-cellular time diversity that is available due to the multipath channel. However, when the channel taps are correlated, this diversity is lost. Although the channel may have many chip resolvable paths, there is not much diversity that the receiver can exploit from them as they are correlated. This

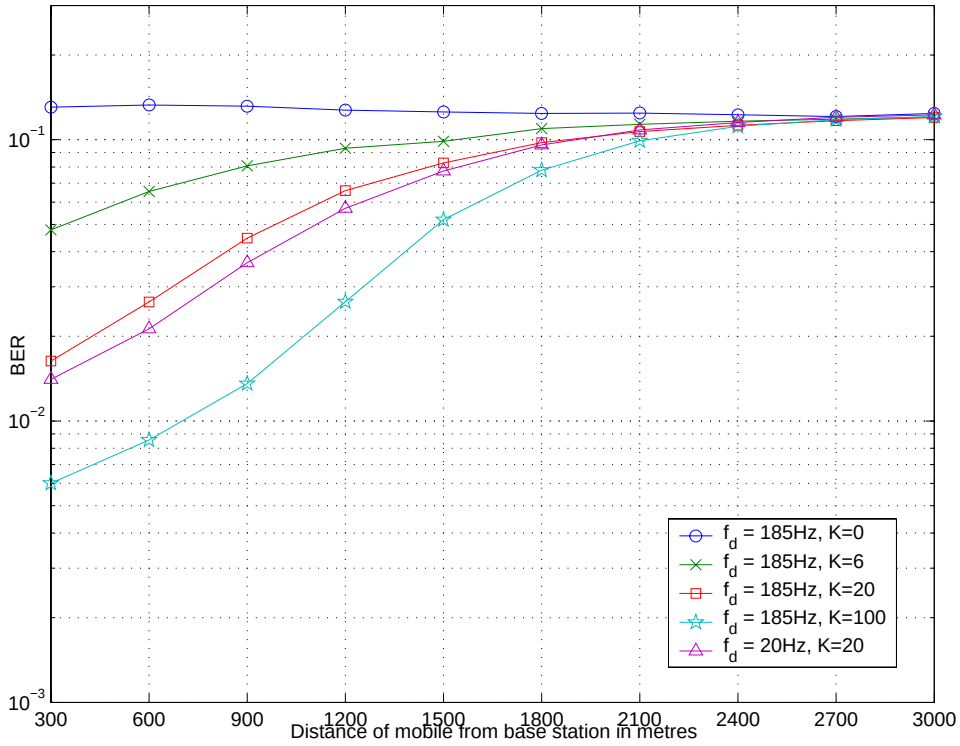

Figure 8. No handoff situation. Channel taps are independent, Rake acceptance threshold = -3dB, Eb/No = 6dB, Tx SIR = -6dB.

is the reason for the poorer BER performance as compared to the independent channel taps case.

Figure 10 also gives us the comparison between chip spaced sampling at the receiver and sub-chip sampling at the receiver. We can see that the performance of a receiver working at $Tc/2$ is better than a receiver working at Tc. There are two main reasons for this. In the case of independent channel taps, the receiver working at $Tc/2$ is able to pick more diversity from the channel as it can detect strong taps even if they are spaced less than a chip. The second reason is common to both independent as well as correlated channel taps. In our channel model, we have assumed the channel to be discretized in steps of $0.01Tc$. Therefore, a receiver working at $Tc/2$ can have a channel estimate which is closer to the original channel than the estimate from a receiver working at Tc. This helps greatly in improving the BER performance.

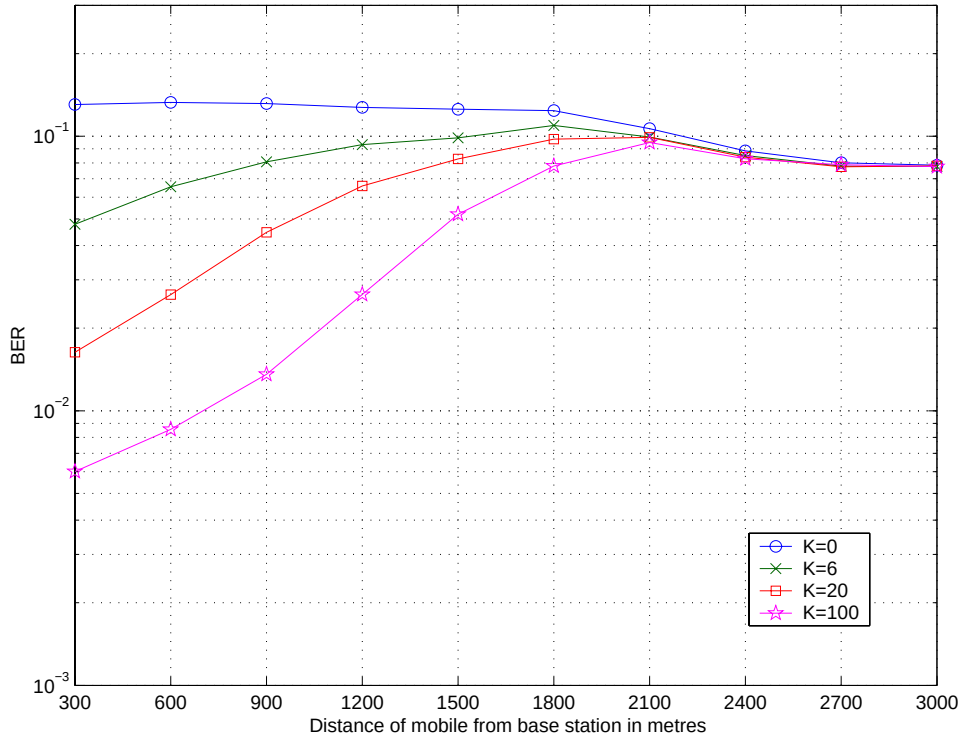

Figure 9. Soft handoff situation. Channel taps are independent, Rake acceptance threshold = -3dB, Eb/No = 6dB, Tx SIR = -6dB.

E. Effect of Pilot cancellation and the Rake finger acceptance threshold

The pilot cancellation block as described in section II-C.2 was implemented. It was observed that when the strength of the pilot channel equalled that of the strength of the traffic channel, the effect of pilot cancellation could not be observed. In fact, in some cases the performance was slightly worse with pilot cancellation.

When the pilot strength was increased to 10dB above the traffic channel strength, the effect of pilot cancellation was pronounced. In IS-95, the pilot channel usually has 30% of the total downlink power, and it defines the coverage region of the cell. Therefore, this assumption of $10dB$ more power in the pilot is reasonable. Since the pilot channel contributed to considerable interference, the BER performance improved greatly when pilot cancellation was performed. This can be observed in Figure 11 where the BER curves have been plotted with and without pilot cancellation. The threshold for accepting

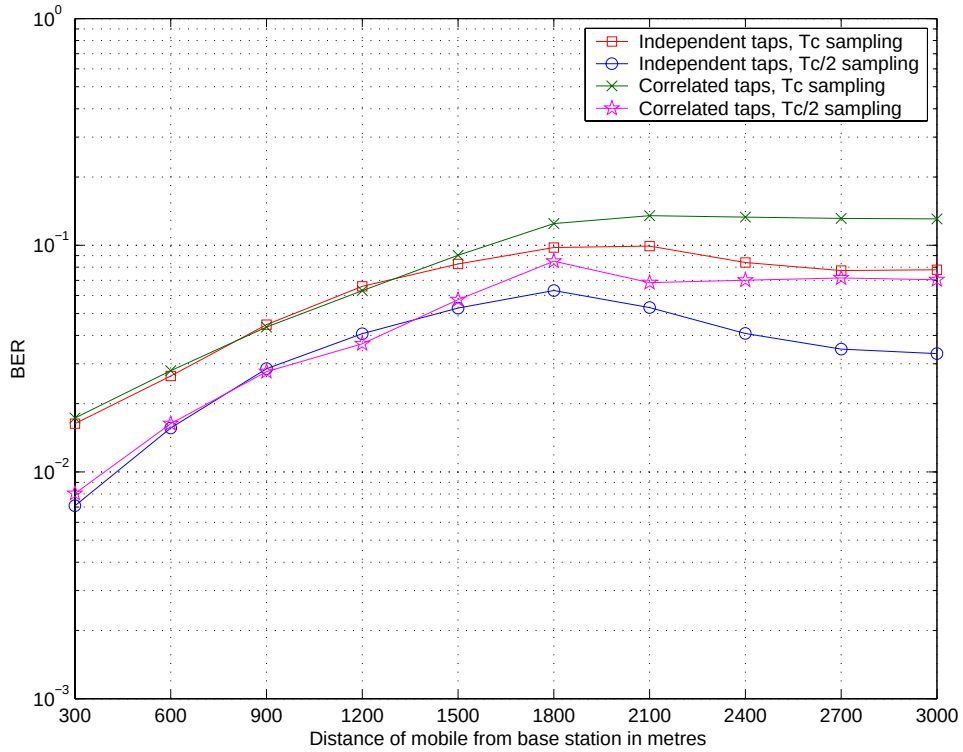

Figure 10. Comparison of BER performance with correlated/independent channel taps & $Tc/\frac{Tc}{2}$ sampling at the receiver. Rake acceptance threshold = -3dB, Eb/No = 6dB, Tx SIR = -6dB.

Rake fingers during channel estimation has been fixed at -3dB.

When the threshold for accepting Rake fingers during channel estimation is decreased to -6dB, the BER performance improves as shown in Figure 12. The reason for this is as follows. During the Rake combining, combining strong paths will help in improving performance. At the same time, including weaker paths, which may be spurious might hamper the performance. Therefore, a threshold of -3dB was set for accepting Rake fingers during channel estimation. Such a sharp threshold might help in improving the performance near the base station where there is not much time diversity and there is a higher chance of spurious paths. However, the same threshold might cause genuine taps to be excluded at distances farther away from the base station. Therefore, decreasing the threshold for accepting Rake fingers to -6dB helps in such a situation. Also, the improvement in the BER performance due to pilot cancellation is higher when the Rake

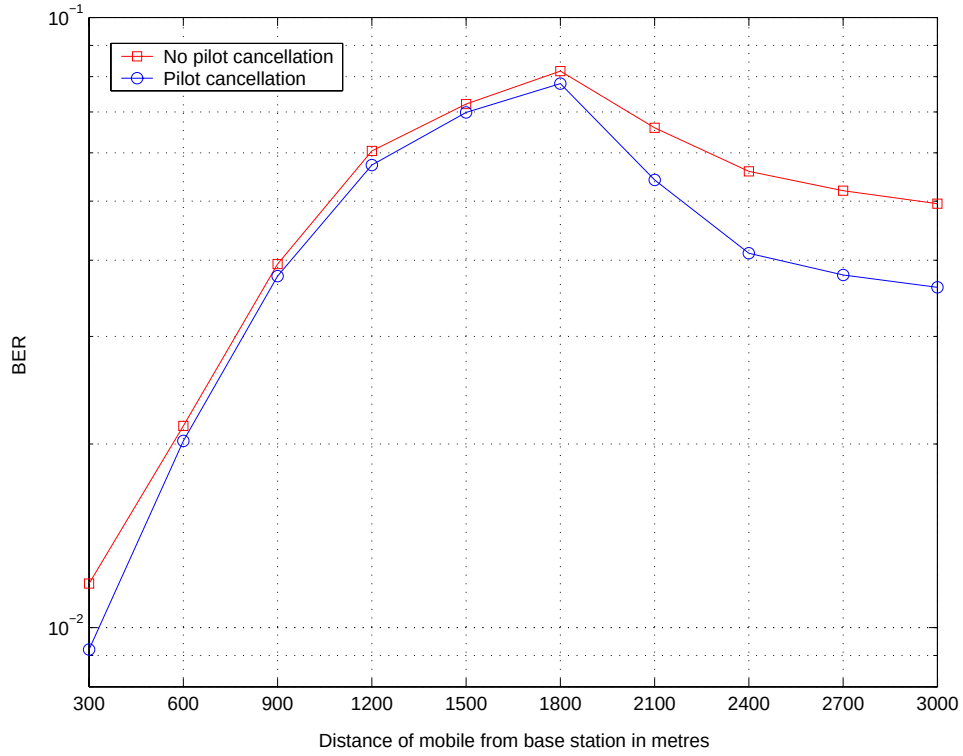

Figure 11. The improvement in BER with pilot cancellation. Rake acceptance threshold = -3dB . Soft handoff, Independent channel taps & $\frac{Tc}{2}$ sampling at the receiver. Eb/No = 6dB, Tx SIR = -9.5dB.

threshold is -6dB than when it is -3dB.

In our simulations we also increased the channel estimation window from 256 chips to 1024 chips but the improvement in BER was marginal. Hence, we have shown all the results for a channel estimation window which is 256 chips in length.

IV. Conclusion

We implemented a simulator for the downlink of a DS-CDMA system and investigated the BER performance of the RAKE receiver as a function of the distance of the mobile from the base station. Various models were proposed to model the delay spread in the channel, correlated channel taps and the line of sight component of the channel. Based on the simulation results, we can make the following conclusions.

1) There are a combination of effects which come into play while determining the

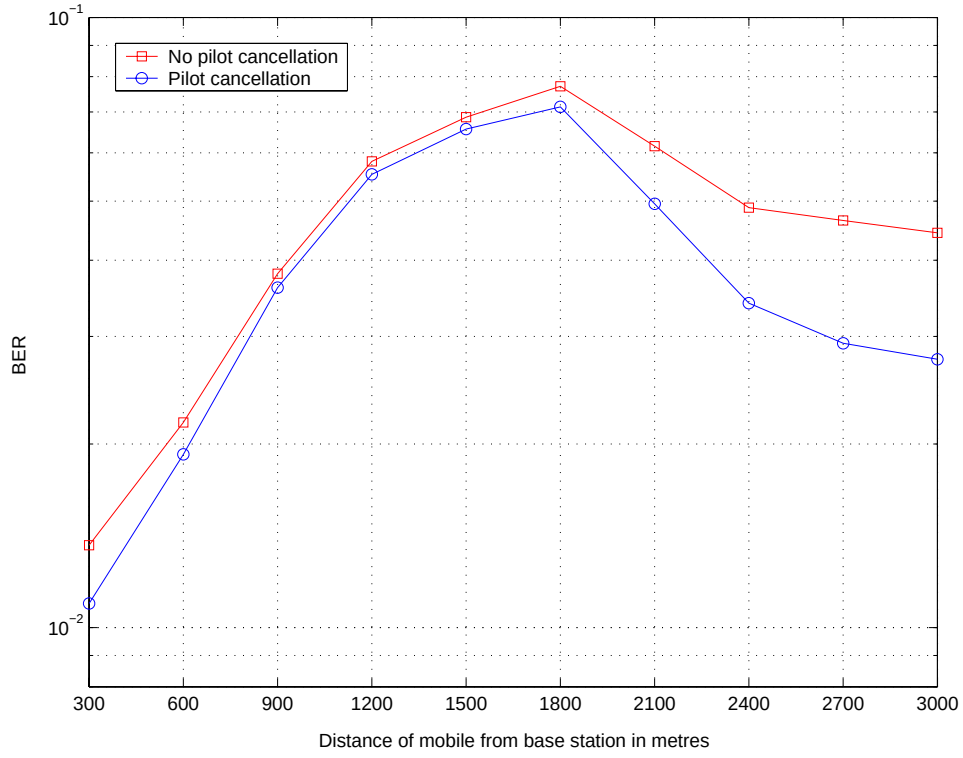

Figure 12. The improvement in BER with pilot cancellation. Rake acceptance threshold = -6dB . Soft handoff, Independent channel taps & $\frac{Tc}{2}$ sampling at the receiver. Eb/No = 6dB, Tx SIR = -9.5dB.

performance of a DS-CDMA system. The presence of a line of sight component in the multipath channel helps tremendously in improving the BER performance especially at distances close to the base station where the LOS component has sufficient strength as compared to the NLOS components. In fact this LOS component can overcome the lack of time diversity due to correlated fading, at distances close to the base station.

2) We find that the macro-cellular diversity obtained due to soft handoff plays an important role in reducing the BER near the edge of the cell site. In the presence of uncorrelated channel taps, there is some micro-cellular diversity that the RAKE receiver can make use of. But this diversity seems to be inadequate as the BER performance becomes poorer with increasing distance when the mobile is not

in hand off. This is due to the inability of the receiver (working at chip-rate or twice chip-rate) to synchronize to a channel which is arbitrarily spaced. This not only causes loss of orthogonality but also introduces some correlation among the various estimated taps. The soft handoff situation, on the other hand, leads to improved performance as an independent copy of the signal is received from another base station.

3) However, the micro-cellular diversity is not to be ignored. We find that when the channel is modelled to have correlated taps, the performance is much worse when compared to a channel having independent taps. Therefore, there is some amount of diversity advantage that is obtained due to the multipath channel, although it may not be very prominent.
4) It was also observed that when the receiver worked at twice the chip rate, the BER performance was better than when the receiver worked at chip rate. The main reason for this is that the receiver is better “matched” to the channel, and can pick some strong taps in the channel which were previously missed out due to chip rate sampling.
5) The effect of pilot cancellation was investigated and it was observed that pilot cancellation at the receiver helped in improving the performance when the pilot channel was much stronger than the traffic channels. Also, it was observed that the a 6dB threshold for RAKE finger acceptance led to better performance than a 3dB threshold. This is especially true at distances farther away from the base station.

To our knowledge, many of these results are new, and have not appeared in open literature. It is hoped that these results will be useful to practising DS-CDMA engineers, and also help in designing handoff thresholds and coverage designs for cellular networks.

It will be interesting to extend this work to Transmit diversity DS-CDMA downlink connections, and also incorporate the effect of Orthogonal Variable Spreading Factor

(OVSF) codes. Future research will be to perform similar studies with a Generalized RAKE (GRAKE)[5] or an Equalizer at the receiver in place of the traditional RAKE structure. The Equalizer will definitely lead to a better performance but will lead to increased complexity and the receiver will have to know the particular shift on the PN sequence that has been assigned to the mobile. A GRAKE is a trade-off between the RAKE and an equalizer in terms of complexity as well as performance.

REFERENCES

1. E H Dinan and B Jabbari, Spreading Codes for Direct Sequence CDMA and Wideband CDMA Cellular Networks, *IEEE Communications Magazine*, September 1998.
2. J C Liberti Jr., T S Rappaport, *Smart antennas for wireless communications: IS-95 and third generation CDMA applications*, Prentice Hall, 1999.
3. F Alam, Simulation of Third Generation CDMA Systems, *MS Thesis, Virginia Polytechnic Institute & State University*, 1999.
4. D J Young, N C Beaulieu, The Generation of Correlated Rayleigh Random Variates by Inverse Discrete Fourier Transform, *IEEE Transactions on Communications*, vol. 48, pp. 1114-1127, July 2000.
5. G E Bottomley, T Ottosson, Y E Wang, A Generalized RAKE Receiver for Interference Suppression, *IEEE Journal on selected areas in communications, Vol. 18, No. 8*, August 2000
6. J G Proakis, *Digital Communications - 4th edition*, McGraw-Hill, 2001.
7. T S Rappaport, *Wireless Communications: Principles and Practice*, Pearson Education Asia, 2002.
8. A Scherb, V Kuehn and K Kammeyer, Pilot Aided Channel Estimation for Short-Code DS-CDMA, *IEEE Seventh International Symposium on Spread Spectrum Techniques and Applications* , 2002
9. S Jagannathan, Studying the Effect of Delay Diversity on a DS-CDMA Downlink, *B.Tech. Thesis, Indian Institute of Technology, Madras*, 2003.

LIST OF FIGURES